Boye CB *et al.* (2025)
Nova Geodesia 5(1):303
Research Article

Shoreline predictive model using artificial intelligence for the homogeneous beach of the Western Coast of Ghana

Cynthia Borkai BOYE*, Peter Ekow BAFFOE, Paul BOYE

University of Mines and Technology, Tarkwa, Ghana;
*cboye@umat.edu.gh (*corresponding author); pebaffoe@umat.edu.gh; pboye@umat.edu.gh*

Abstract

Coastal areas are preferred home to about 40% of global population than any other ecosystems. Many organisms, including endangered species, live along sandy beaches. Nonetheless, such beaches are prone to erosion and flooding owing to natural and human factors. The shoreline, where land meets the sea, is highly dynamic and challenging to predict with accuracy. Existing predictive numerical models rely on multiple parameters, while statistical analysis of historical shoreline positions assume a linear distribution, overlooking the nonlinear nature of the data. This present study explored the application of nonlinear approaches like artificial neural networks (ANN) and other artificial intelligence techniques to predict shoreline change rate along the sandy beach of the study area using recurrent neural networks approaches: nonlinear autoregressive neural network (NARNN) and nonlinear autoregressive exogenous neural network (NARXNN); backpropagation neural network (BPNN), and compared results with multiple linear regression (MLR) model. Data used was partitioned into two: 70% was used for training and 30% was reserved for evaluating the performance of the models. From the developed models the output forecast for shoreline change were determined. NARXNN yielded best prediction, followed closely by NARNN and then BPNN as against MLR model. The optimum model developed for shoreline prediction provides invaluable information for planners and engineers of the coast.

Keywords: nonlinear autoregressive neural network with external input; sandy beaches; shoreline dynamics prediction; artificial intelligence

Introduction

Sandy beaches constitute about 33% of global ice-free shorelines, of which 24% are eroding, 28% accreting, and the remaining shorelines are stable (Luijendijk *et al.*, 2018). The stability of beaches depends on several natural and human-induced factors such as wave climate, tides, relative sea level rise, interference with natural coastal processes, and damming of fluvial sources that nourish the shores among others. About 40% of humans reside in coastal areas worldwide due to its favourable climatic conditions, opportunity for fisheries, and its support for recreational opportunities and tourism, as compared to other ecosystems (Barragan *et al.* 2015;

Received: 16 Jan 2025. Received in revised form: 28 Feb 2025. Accepted: 01 Mar 2025. Published online: 01 Mar 2025.

Defeo *et al.*, 2009). Sandy beaches, on the other hand form habitat for many organisms including shorebirds, crustaceans, mollusks, and even threatened creatures like sea turtles, which nest their eggs in the dry sandy beaches (Schlacher *et al.*, 2014; Defeo *et al.*, 2009). Generally, coastal land has high economic value in as much as most cities and industrial areas, particularly those in West Africa, are sited along the coast and this explains the skewness of population distribution along coastal zones. Nevertheless, sandy beaches are susceptible to erosion and flooding, besides, the position of the shoreline varies and are difficult to predict accurately.

Knowledge and understanding of the dynamics of the shoreline along a given coast is vital for making informed decisions by coastal planners, engineers, and other stakeholders. Existing shoreline change predictive models have been used in the past, popular among these are the Generalize Model for Simulating Shoreline change (GENESIS), the Soft Cliff and Platform Erosion (SCAPE), Long-Term Configuration (LTC), and the numerical shoreline change model based on the Preissmann Schematic Technique (COPREM-2D). While the GENESIS and the SCAPE simulate future shoreline evolution trends using several input parameters, some of which are not readily available, the LTC models determine long-term shoreline evolution by considering the drivers of future shoreline change, computation of the coastal evolution and final post-process stage (Alvarez-Cuesta *et al.,* 2021). The COPREM-2D model tends to predict long-term changes that coastal structures may have on shorelines (Ulger and Tanrivermis, 2023). Most of these models require several parameters some of which may be scarce, besides they are based on the assumption of energy conservation.

Thomas and Frey (2013), found out that measurements and statistical analyses of historic shoreline positions could be used to accurately determine shoreline change using numerical models. These include the linear regression rate (LRR), end point rate (EPR), and weighted linear regression rate (WLR) among others (Baig *et al.*, 2020; Armenio *et al.*, 2019; Oyedotun, 2014; Ruggiero and List, 2009). Some studies have also confirmed that LRR is an appropriate statistical method for soft shores in some instances, where the shorelines have little or no activities by humans (Zeinali *et al.*, 2021; Maio *et al.*, 2012). However, data stationarity assumption using these traditional methods, for example, auto-regressive moving average (ARMA) is hard to achieve (Sheremetov *et al.*, 2014), besides, human activities along the shoreline are inevitable along most coastal zones. Hence, nonlinear models such as artificial intelligence techniques were explored to predict rate of shoreline change of the study area. The artificial neural networks (ANN) approaches, which draw inspiration from the human brain, have the ability to deal with nonlinearities and time-variability issues in data as it is capable of learning and adapting to changing environments. The ANN assists in meticulous analysis of dimensional data in recent times to model nonlinearities in data through training of the system; it has also proven to be more efficient and faster in operation (Saadon *et al.*, 2024).

ANN has been used to predict coastal dynamics in recent times that yielded promising findings. For instance, sea levels were predicted by the use of nonlinear auto-regressive neural network (NARNN), and the study found that the number of hidden layers chosen affects the accuracy of prediction (Rizkina *et al.*, 2019). Other researchers predicted variability of the shoreline along the Croatian coast based on nourishment demand (Bujak *et al.*, 2021), shoreline variability from surveillance camera images for the Nha Trang Coast in South Central Vietnam (Yin *et al.*, 2021), wind speed forecasting in Malaysia (Sarkar *et al.*, 2019), and Zeinali *et al.* (2021), also predicted shoreline change based on historic data. The results demonstrate the predictive power of ANN. ANN has also been applied in shoreline change studies in some jurisdictions, for example, along five selected beaches in Southern Taiwan, where the performance of different activation functions used in modelling shoreline change were compared in a study using a multilayer perceptron (MLP) neural network (Chen and Wang, 2020). Monthly shoreline changes along the Noor Bay in south Caspian Sea were successfully predicted using backpropagation feed-forward (BPFF) ANN, and the results were validated using shoreline change surveys (Alizadeh *et al.*, 2011). Other deep learning models which learn high-level abstraction from data, have also been applied in shoreline change prediction such as Convolutional deep learning (Gomez-de la Pena *et al.*, 2023) to yield accurate prediction. Recurrent neural networks: NARNN and nonlinear auto-regressive exogenous neural network (NARXNN) have also been successfully applied in shoreline change as well as in other fields of applications (Sheremetov *et al.*, 2014; Rizkina *et al.*, 2019; Jamei *et al.*, 2023).

Shoreline change rates in Ghana have been associated with significant variability and uncertainties (Ankrah *et al.*, 2023; Boye *et al.*, 2018; Evadzi *et al.*, 201; Jonah *et al.*, 2016). This study, therefore seeks to predict shoreline change in the Western Region of Ghana using NARNN, NARXNN, back-propagation neural network (BPNN), and to compare results with multiple linear regression (MLR) model. This is to enable the complexities and uncertainties associated with shoreline input data to be simulated with the machine learning approaches which are capable of recognizing patterns and making inferences from data to produce accurate and reliable forecasts.

Materials and Methods

Study Area

The study area is located between latitudes 4°40′ and 5°10′ North, and longitudes 3°07′ and 1°40′ West. The coastline covers three districts, namely Ahanta West, Elembelle, and Jomoro districts along the Western zones of Ghanaian coast. Its shores stretch over 100 km of uninterrupted sandy beach constituting about 18% of the coastline of Ghana. The topographic elevation of the coast is below the 30 m contour and the beach lies between the Ankobra river estuary near Axim and the Tano river estuary close to the Ghana and Ivory Coast border. The ocean climate along the coast of Ghana exhibits significant wave period from 10 to 12 s and significant wave height of approximately 1.2 m (Boye *et al.*, 2018). The local sea levels rise ranges from 2 to 3 mm/year, and prevailing waves moves in the south-southwest direction (Appeaning Addo, 2014). It is a low-energy coast that comprises gently sloping fine sandy beaches backed by coastal lagoons (Anim, 2019; Yaw Dadson, 2015). The Amunsuri, Ankobra, and Tano rivers deposit their load to nourish the shore of the study area against the powerful west-east long-shore drift (Boye *et al.*, 2022). The Western Region lies on sedimentary marine deposits which is situated in the Tano Basin, underneath Eocene and Cretaceous Appolonian sediments. The Appolonian is made up of rapidly changing layers of sands and clays with isolated flat beds of gravel and fossiliferous limestone (Kesse, 1986). Figure 1 shows an orthophoto Map of the study area.

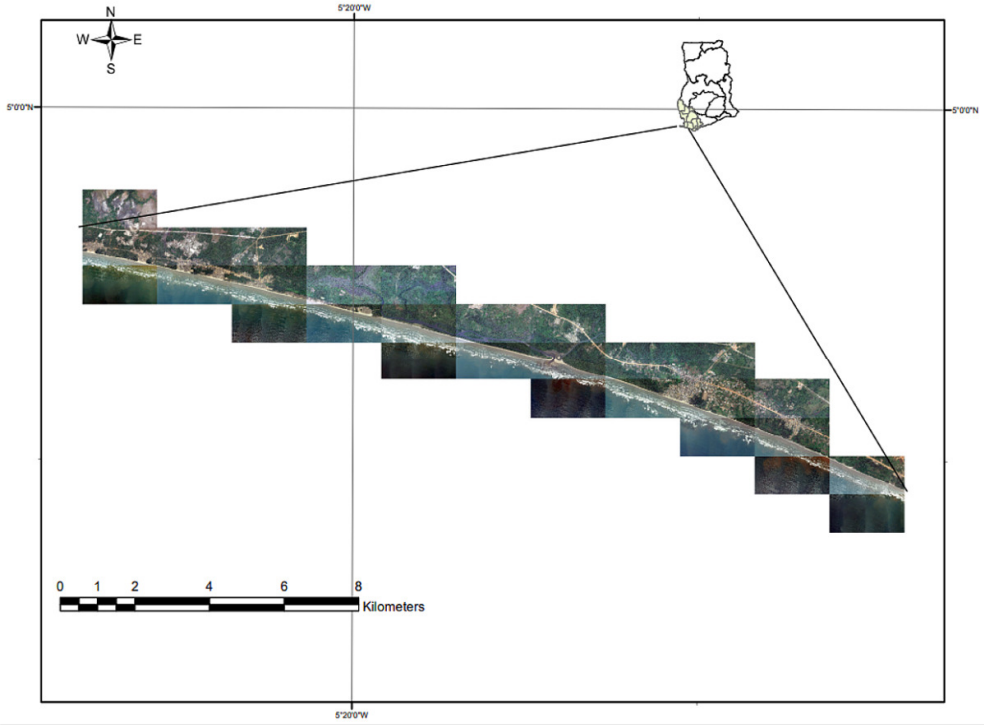

Figure 1. Orthophotography of the sandy beach in the Western Region of Ghana

Methods

BPNN, NARNN, and NARXNN techniques were used for prediction of shoreline in the study. The models developed were compared with the MLR model to determine the best model for predicting shoreline for the area. Figure 2 presents a flowchart of the methods employed to propose the shoreline change predictive model.

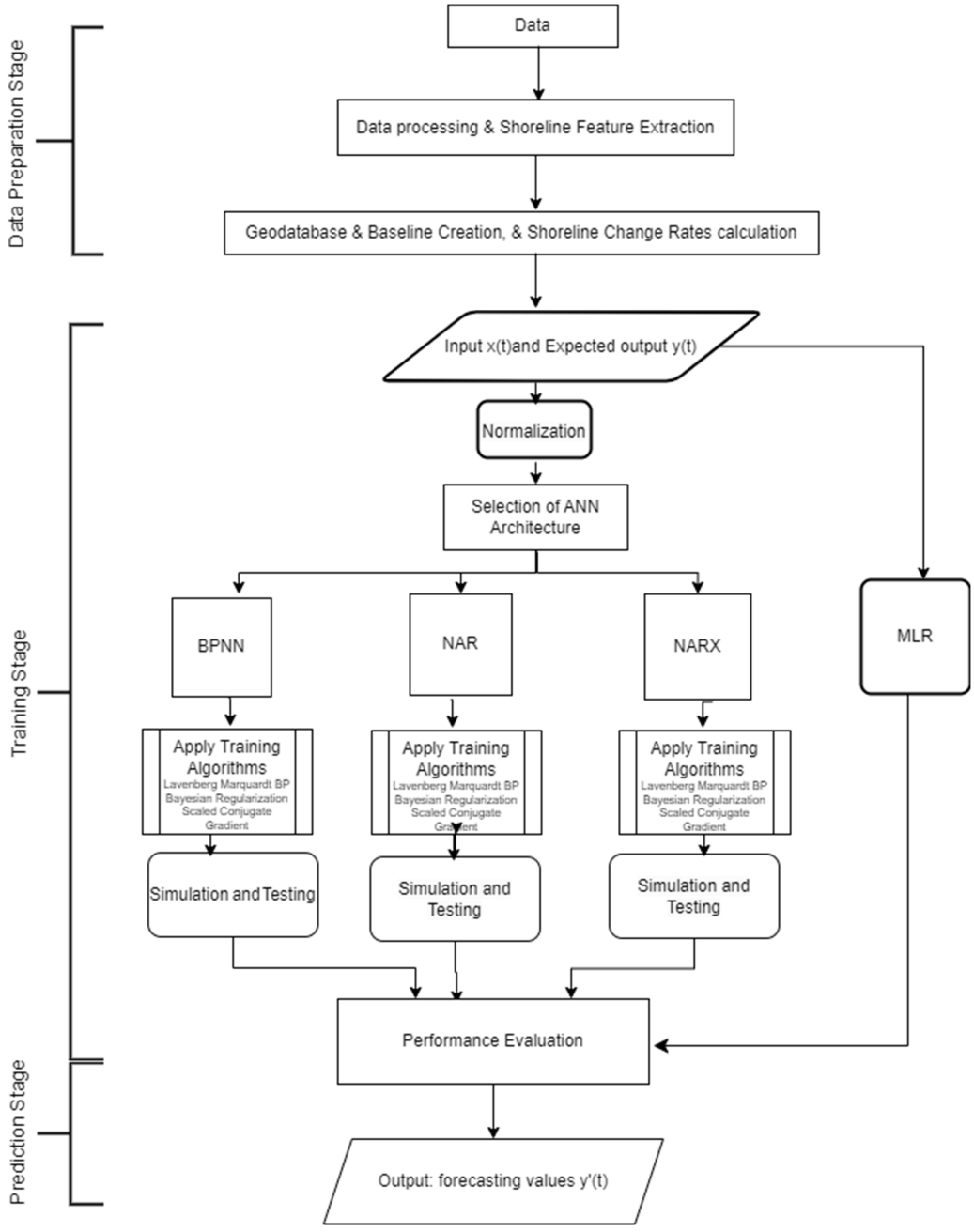

Figure 2. Flowchart of proposed shoreline change predictive model

Backpropagation Neural Network

The BPNN concept was proposed in 1986 by Rumelhart and McClelland (Goh, 1995) within the framework of the ANN algorithm, and it employs nonlinear neuron processing functions. Computational units, neurons, are used to identify correlations and patterns between input and output variables (Dodo *et al.*, 2024; Khairudin *et al.*, 2024). It is a feed-forward supervised learning algorithm mostly used to resolve regression and classification troubles. It comprises primarily input layer, hidden, and output layers respectively. Each link between two neurons in any two layers represents adjustable weights and biases of the neural network which is based on the error between the predicted and the actual outputs. The training algorithm of the BPNN operates in two phases: forward and backward propagation.

The forward propagation involves forward pass of input and error calculations *(*i.e., difference in targeted output and output predicted) and the backward propagation involves computed error propagated backwards through the network to the layers and the weights are adjusted. The process continues until an acceptable level of error is obtained (He *et al.*, 2024).

The weights and biases of each neuron in the network are updated by the algorithm using the gradient descent optimisation method. The gradient descent method determines the slope of the error function with respect to the weights and biases, then updates these parameters in the direction of the negative gradient to minimize the error (Rastgou *et al.*, 2024). Figure 3 shows the BPNN topology which is one of the most successfully used neural network techniques in many real-world applications (Nayak *et al.*, 2014).

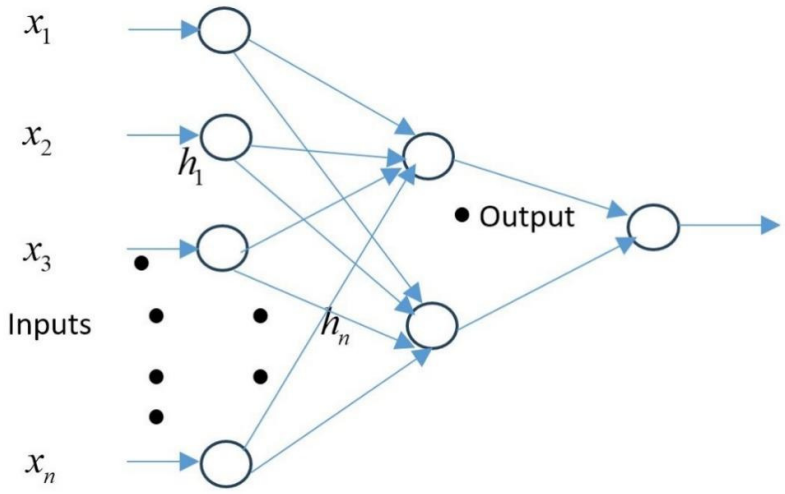

Figure 3. Backpropagation Neural Network Topology

The study used the sigmoid activation function for the backpropagation algorithm as shown in Equations (1) and (2). It is the most frequently used activation function, although the step, linear, ramp, or hyperbolic tangent functions could also be used (Jeyanthi and Subadra, 2014).

$$F(x) = \frac{1}{1 - e^{-sum}} \tag{1}$$

Where, $sum = \sum_{i=1}^{n} (x_i w_i)$ (2)

Nonlinear Autoregressive Neural Network

The NARNN is an ANN approach used for multi-step ahead predictions for time series data. It is a multi-layered feed-forward neural network which comprises three or more layers. The structure comprises input and output layers with a hidden layer in-between them (see Figure 4). Studies have shown that a single

hidden layer is sufficient for nearly all applications on condition that the number of neurons is adequate (Ahmed and Khalid, 2017). The hidden layer is made up of neurons (π) which aggregates all the input signals (δ), and the weights accordingly, to generate an activation pattern.

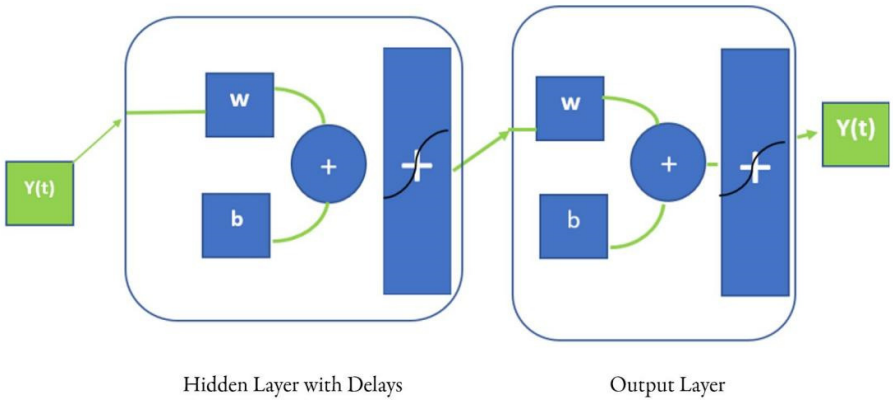

Figure 4. NARNN Topology

In this study, the NARNN was trained with the Levenberg-Marquart backpropagation training algorithm. This training algorithm is considered to be the quickest backpropagation algorithm since it bypasses the Hessian matrix computation that go through large computation time; rather it depends on second-order derivative approximation (Saba and Elsheikh, 2020).

Every neuron of the hidden layer derives its activation signal from the weighted sum in the inputs. The hidden layer of the τ^{th} neuron is computed to give an output based on Equation (3) (Saadon *et al.*, 2024; Ahmed and Khalid, 2017):

$$\pi\pi_{\tau} = \sum_{\iota=0}^{\delta} \left(x_{\iota} w_{\iota\tau} \right) \qquad \left(\iota = 0,\ldots,\delta; \quad \tau = 1,\ldots,\pi \right) \tag{3}$$

Where, $w_{\iota\tau}$ is the link weights vector between the input node ι and hidden node τ, and x_{ι} represents the input vector. The activation value of each neuron is processed through an activation function, g . As a result, the output z of τ^{th} neuron is computed as shown in Equation (4).

$$z_{\tau} = g\left(\pi\pi_{\tau} \right) \tag{4}$$

The outputs obtained are fed into the single neuron of the output layer to compute the last output as shown in Equation (5):

$$\hat{y}(t) = g_0 \left(\sum_{\tau=0}^{n} \left(z_{\tau} w_{\tau k} \right) \right); \quad \left(\tau = 0,1,\ldots,n \right) \tag{5}$$

Where, t indicates time, g_0 is a line function utilised as output layer activation, and $w_{\tau k}$ is the link weight between the hidden node τ and output node k .

During the training process, both the number of neurons in the hidden layer and the synaptic weights connecting different neurons are adjusted to achieve an optimal NARNN structure that maximizes forecasting accuracy. Usage of low number of neurons may negatively affect the accuracy of computation and generalisation ability of the model, while usage of higher number of neurons may increase the costs of model computation that may result in data over-fitting.

Figure (5) shows the NARNN structure and its mathematical representation could be presented as in Equation (6) (Zu and Zhang, 2022; Saba and Elsheikh, 2020):

$$y(t) = g\left(y(t-1),...,y(t-d)\right) + \varepsilon(t) \tag{6}$$

Where, $y(t)$ represents the current response, t indicates time, g being the function, d the number of network delays, and $\varepsilon(t)$ represents the error term.

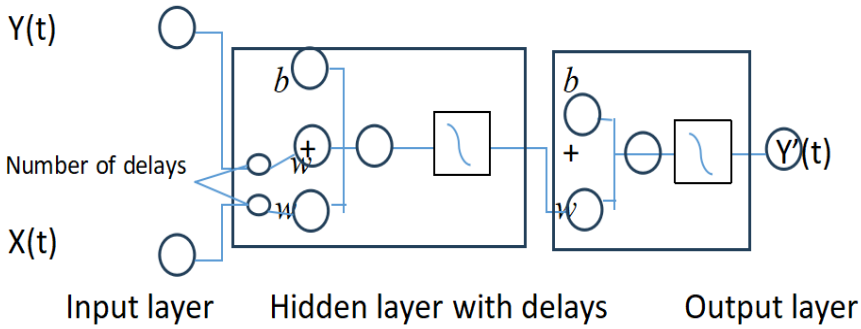

Figure 5. NARXNN Topology

The estimated model is represented as shown in Equation (7) (Zu and Zhang, 2022):

$$\hat{y}(t) = \alpha_0 + \sum_{\tau=1}^{k} \alpha_\tau \phi\left(\sum_{\iota=1}^{d} \beta_{\iota\tau}\, y_{t-\iota} + \beta_{0\tau}\right) + \varepsilon(t) \tag{7}$$

Where, k is the number of hidden layers with the transfer function ϕ, $\beta_{\iota\tau}$ parameter corresponds to the weight linking the input unit ι and the hidden unit τ, whereas α_τ represents the weight linking the hidden τ and the output units, $\beta_{0\tau}$ and α_0 are the related constants, in respect of the hidden τ and output units, and $\varepsilon(t)$ is the error term.

Nonlinear Autoregressive Exogenous Neural Network

The NARXNN, a multilayer neural network model, incorporates nonlinear auto-regressive exogenous inputs that are well suited for the prediction of time series and nonlinear systems modeling. The model structure consists of 3-layers: an input, hidden, and output which are interlinked by weighted connections and are activated through a transfer function that fires when powerful inputs are recorded (Saadon *et al.*, 2024) (see Figure 5).

The neurons in all layers are summation of the current input vector (x_ι) supplied by the preceding layer and weights vector ($w_{\iota\tau}$) to produce the scalar multiple ($x_\iota . w_{\iota\tau}$). The resulting ι^{th} neuron of the layer is estimated from Equation (8) (Shen *et al.*, 2023):

$$y_\iota = f\left(\sum_{\tau=1}^{n} (x_\iota . w_{\iota\tau})\right) \tag{8}$$

Where, f is a nonlinear transfer function and τ represents the input index. In addition, to improve the network convergence, bias (b) connections were added.

Comparing the NARXNN to feedforward artificial neural network, shows some advantages which includes: more effective learning for NARXNN networks as the gradient descent is better; due to the process feedback, the network converges much quicker and generalise better than some other networks (Saadon *et al.*, 2024; Sheremetov *et al.*, 2014). The model of NARXNN raises its sensitivity to historical data, thus improving accuracy of prediction by integrating a time delay with an output feedback delay unit within the input layer of the network. The output of the model is fed back into the input for a specific number of time steps in the case of long-term prediction. As such, the components of the previous regressed input make up the actual sample points in the time series which are step by step replaced by predicted values (Shen *et al.*, 2023).

Consequently, Equation (9) shows the estimated NARXNN network model output at the time t (Sheremetov *et al.*, 2014):

$$\hat{y}(t) = f\left(x(t-1),...,x(t-dx), y(t-1),..., y(t-dy)\right) \tag{9}$$

Where, $x(t)$ is the input at a time t, dy and dx are the memory delays for the feedback and input delays respectively. Both dy and dx should be greater than or equal to 1 while $dx \geq dy$.

Multiple Linear Regression Analysis

The MLR approach depicts ways by which multiple input (independent) variables influence an output (dependent) variable. In the present study, this statistical method was employed to estimate the correlation between two or more shoreline parameters collected from the field that have cause-effect relationship and utilised as input to develop the MLR model to predict changes in shoreline positions (Martin, 2022). Thus, the multivariate regression analysis model estimates the association between the independent variables and the dependent variables synchronically. Practically, some limitations exist with regression models in some field of application for various scenarios (Hesamian *et al.*, 2024). The following are the assumptions that are established for the MLR. First and foremost, there is an assumption of linear relation between the response and explanatory variables. Next, there is only one dependent linear variable. Thirdly, the residuals are normally distributed. Finally, no multicollinearity should exist in the independent variables (Huang *et al.*, 2024). The MLR model is formulated as shown in Equation (10) (Ozgoren *et al.*, 2012):

$$f_i(x) = \beta_0 + \beta_1 x_1 ... + \beta_n x_n + \varepsilon; \quad i = 1,...,n. \tag{10}$$

Where, $f_i(x)$ is the dependent variable observed in MLR, $x_i's$ are the independent variables, $\beta's$ are unknown regression coefficients to be estimated, and ε is the error term. Using the least squares method, the regression estimates in the MLR model are obtained as shown in Equation (11):

$$\hat{f}_i(x) = \hat{\beta}_0 + \hat{\beta}_1 x_1 ... + \hat{\beta}_n x_n + \varepsilon; \quad i = 1,...,n. \tag{11}$$

Where, $\hat{f}_i$ represents the parameters of the response variables in the MLR, $\beta's$ are regression coefficients, and ε is the error term.

Data Used and Models Development

Data Used

Primary and secondary datasets were used for the study. The primary data was obtained from field measurements using Global Position System (GPS) receivers. Differential GPS technique was adopted in the collection of the shoreline positions (2020) by utilising the high water line (HWL) as proxy. Secondary data used included a time series spatial dataset (1974 and 2005) comprising topographic data and orthophotos obtained from the Lands Commission of Ghana. Employing Digital Shoreline Analysis System (DSAS), an

extension of ArcGIS, the shoreline dataset and baseline were created and stored in a personal Geodatabase. The shoreline data of the study area was digitized from a topographic map (1974) and orthophotos (2005) and their reliability for use was assessed (Boye e*t al.*, 2018; Boateng, 2012; Addo *et al.*, 2008). The DSAS was used to cast transects and to calculate the rate of change of the shoreline using End Point rates and linear regression approaches (Legates and McMabe, 2013; Moussaid *et al.*, 2015; Nandy *et al.*, 2017) to produce input and expected output data (target) for the development of the shoreline prediction models.

The multi-temporal shoreline data were extracted from the 2020, 2005 and 1974 datasets, that is, X coordinates, Y coordinates, and date of observation of the shorelines positions were used as independent parameters while change rates were used as response variables (Figure 1). Summary of data used for development of the models is shown in Table 1.

Table 1. Summary of data used

Statistic	X Coordinates (m)	Y Coordinates (m)	Date (year)	Change rate (m/year)
Mean	92987.0700	36039.40	1994.717	1.8231
Minimum	40851.3500	46985.12	1974.086	3.8800
Maximum	133632.3500	25404.19	2020.629	-0.2400
Standard deviation	742369435.7000	35363678.48	336.470	0.8901

Model Building Framework

The variables for the model input and target were initially selected and partitioned appropriately. To ensure uniformity, data scaling was done through the process of normalisation. The step was followed by training of networks until termination standards were observed and the optimal model was obtained and comparison made with the MLR model. The best model was thereafter subjected to testing using selected performance indicators calculated using the input parameters and the predicted shoreline change rates.

Optimum Model development

The NARXNN emerged the best trained model in the study with a structure composed of 3- inputs, 20- hidden neurons, 1- output and a network delay of 4. Similarly, the optimum model of the NARNN that yielded best performance comprises 3- inputs, 10- hidden neurons and 1- output parameters with a network delay of 3. The optimum model for the BPNN had a structure consisting of 3- inputs, 87- hidden neurons and 1- output, that is [3-87-1].

Data Specification and Variable Selection

The various AI models were developed using 2,115 data points. The shoreline positions and dates of observation served as the independent variables, and the computed change rates served as the dependent variables. About 70% (1480) of the data points were used for training in order to develop the AI prediction models while close to 30% (635) of the data points were used to validate the developed models. The partitioning of the data points adopted the commonly used hold-out cross-validation approach. Summary of the data used showed in Table 1.

Normalisation of Data

Prior to the model development process, the input dataset was brought to the same scale by normalising the dataset into an interval suitable for the activation function using the means and standard deviations. Normalisation is a basic data preprocessing measure that facilitates learning from data prior to modeling with ANN (Nayak *et al.*, 2014). Data normalisation standardises data to appear similar across all records and fields, this process scales all data points, making them contribute impartially in the gradient descent process for the optimisation process to converge faster. The normalisation process also allows clean data to be produced for model development. The normalised data is shown in Table 2.

Table 2. Normalised data

Statistic	X Coordinates (m)	Y Coordinates (m)	Date (year)	Change rate (m/year)
Mean	0.5619	0.4928	0.4433	0.5008
Maximum	1	1	1	1
Minimum	0	0	0	0
Standard deviation	0.0862	0.0759	0.1553	0.0525

Training of Networks

During modelling with ANN, the data points were structured in order to provide the desired output for a specific input. In a similar vein, the ANN algorithms were also trained in this study to determine the functional relation existing between the independent parameters (input) and the response parameters (output). The network training was performed using the 2,115 data points partitioned into 1,480 (training) and 635 (testing) subsets. The training set enables the parameters to be used to express the state of the model through minimisation of the error function, while the testing set allows for validation of the model. The Levenberg–Marquardt back-propagation algorithm was used during the network training of the BPNN. Also, the Bayesian Regulation and Scaled Conjugate Gradient learning algorithms were employed to train the NARNN and NARXNN respectively while varying the number of neurons and delays (see Tables 3 and 4).

Table 3. Results of varying training algorithms, neurons and network delay parameters for NARNN

Training algorithm	No of neurons	Delay	Training		Testing		No of iterations
			MSE	R	MSE	R	
Levenberg Marquardt	10	2	0.00174	0.9835	0.00206	0.978	25
Bayesian Regulation	10	2	0.00191	0.9815	0.00000	0.000	148
Scaled Conjugate Gradient	10	2	0.00194	0.9807	0.00182	0.9822	84
Levenberg Marquardt	20	2	0.00176	0.9829	0.00227	0.9766	16
Levenberg Marquardt	20	3	0.00197	0.9810	0.00155	0.9850	30
Levenberg Marquardt	10	3	0.00180	0.9830	0.00175	0.9820	12
Levenberg Marquardt	20	2	0.00176	0.9829	0.00227	0.9766	16
Levenberg Marquardt	20	3	0.00197	0.9810	0.00155	0.9850	30
Levenberg Marquardt	20	4	0.00174	0.9836	0.0025	0.9760	11

Table 4. Results of varying training algorithms, neurons and network delay parameters for NARXNN

Training algorithm	No of neurons	Delay	Training		Testing		No of iterations
			MSE	R	MSE	R	
Levenberg Marquardt	20	2	0.00170	0.9800	0.00154	0.9857	34
Bayesian Regulation	20	2	0.00167	0.9840	0.00000	0.0000	100
Scaled Conjugate Gradient	20	2	0.00180	0.9825	0.00167	0.9842	56
Levenberg Marquardt	20	3	0.00152	0.9850	0.00219	0.9803	19
Bayesian Regulation	30	3	0.00168	0.9840	0.00000	0.0000	237
Scaled Conjugate Gradient	20	3	0.00190	0.9820	0.00125	0.9876	77
Levenberg Marquardt	20	4	0.00163	0.9850	0.00190	0.982	10
Levenberg Marquardt	20	5	0.00159	0.9850	0.00211	0.9803	12
Levenberg Marquardt	30	3	0.00164	0.9840	0.00156	0.9844	17
Levenberg Marquardt	30	4	0.00160	0.9850	0.00217	0.9801	9

The networks in this stage were allowed to train until no significant improvement occurred. Thereafter training of the networks, testing was done using unseen data to provide an independent evaluation of the performances of the BPNN, NARNN, and NARXNN. The MSE values of the models were monitored closely at each stage of training and testing to help in the determination of the optimum model. Additionally, other indicators such as correlation coefficient (R) and coefficient of determination (R^2) were also used to adjudge the ANN models performances. The models that yielded the highest R and R^2 values, as well as the lowest MSE, after several experiments were compared with that of MLR model (Nandy *et al.*, 2013).

Models Performances Evaluation

During the model performance evaluation in this study, the root mean square error (RMSE), the Percentage root mean square error (PRMSE), the RMSE observations standard deviation ratio (RSR), the Legates and McCabe's (ELM) and the Mean absolute percentage error (MAPE) were used (Tian *et al.*, 2016; Legates and McMabe, 2013; Willmott *et al.*, 2006) as statistical indicators to ascertain the efficiency of the models developed for the shoreline change prediction.

• Root Mean Square Error

The RMSE is a dimensional statistic which measures the average difference between predicted and actual values of a statistical model. The metric is often used to assess the accuracy of parameter estimates and expresses the mean error of a prediction model in terms of units of the variable under consideration (Equation 12).

$$RMSE = \sqrt{\frac{\sum_{j=1}(O_j - P_j)^2}{\tau}} \quad (12)$$

Where, τ is the number of data points, and O and P are the measurement and prediction values respectively.

• Percentage Root Mean Square Error

The PRMSE is a scale-independent statistic which is able to assess the precision of the performance of a predictive model (Equation (13).

$$PRMSE = \frac{RMSE}{x_m} * 100 \quad (13)$$

Where, x_m is the mean observed value.

• RMSE Observations Standard Deviation Ratio

The RSR is a standardise form of RMSE which is a measure of the variability of the observations. Lower value of RMSE value connotes least RSR value which represents, better power of prediction of the developed model (Equation 14).

$$RSR = \frac{RMSE}{S_d} = \frac{\sum_{i=j}^{\tau}(O_j - P_j)^2}{\sum_{i=j}^{\tau}(O_j - O_m)^2} \quad (14)$$

Where, S_d represents the standard deviation of the measurements, τ is the number of observations, O and P are the observations and prediction values, respectively. O_m represents the average of the observation values.

• Legates and McCabe

The ELM is a statistic which evaluates the goodness of fit of the predictive and the observe data. This measure provides the evaluation of the model's predictive abilities. The closer the ELM value to 1 gives an indication of high predictive power of the model developed (Equation 15).

$$ELM = 1 - \frac{\sum_{i=j}^{\tau} Abs(P_j - O_j)^2}{\sum_{i=j}^{\tau} Abs(O_j - O_m)} \quad (15)$$

Where, O and P represents the values of the observations and that of the predicted, respectively, O_m represent the average values of the observations, and τ is the number of observations made.

Assessment of Efficiency the Models Developed

To build the models for accurate predictions, the selected data points were used for training to fit the models and the testing data points were used as an independent data to demonstrate the forecasting capability of the models developed. To predict the shoreline change, the models were assessed by comparing the methods - NARXNN, NARNN, and BPNN - to find how best each method fits the data points, as well as it application for future works. This was done by using the five performance indices RMSE, PRMSE, RSR, MAPE and ELM (Table 5); the accuracy of the models were assessed as shown in Table 6.

Table 5. Training and testing results of the optimum models

AI Model	Training Algorithm	No of neurons	Training		Testing		No of Iterations	Network Delay
			MSE	R	MSE	R		
NARNN	Levenberg Marquardt	10	0.0018	0.9830	0.00175	0.9820	12	3
NARXNN	Levenberg Marquardt	20	0.00163	0.9850	0.00190	0.9820	10	4
BPNN	Levenberg Marquardt	87	0.00310	0.9696	0.00290	0.9723	237	-

Table 6. Summary of accuracy assessments

	R	RMSE	PRMSE	RSR	ELM
BPNN	0.970	0.05564	11.11136	0.059011	0.984621
NARNN	0.9836	0.04334	8.652473	0.035752	0.990679
NARXNN	0.9906	0.04108	8.203724	0.032107	0.969034
MLR	0.562	0.02184	1.19776	0.000535	0.9995

Optimum Model formation, Efficiency and Performance Evaluation

Optimum Model formation

The optimum trained model of the NARXNN had a model structure comprising three inputs, twenty hidden neurons, one output and a network delay of 4. Similarly, the optimum model of the NARNN that produced the best performance had three inputs, ten hidden neurons and one output parameters with a network delay of 3. The optimum model for the BPNN had a structure consisting of three inputs, eighty-seven hidden neurons and one output, that is [3-87-1].

Model Efficiency Assessment

Tables 5 and 6 present the training and testing results of the optimum models produced as well as summary of the accuracy assessment of the models developed.

Model Validation using existing recent research findings

It is crucial to validate the results of this study with findings of research works found in literature in order to guarantee the reliability and credibility of the study. A careful a review of literature from 2020 to 2024 was undertaken and represented in Table 7.

Taking into consideration the range of data set used, the choice of input variables and the AI model utilised, variations exist from one study to the other with each study using different error metrics for model performance evaluation. Therefore, commonly used indicators were selected for the validation. For example, Kumar (2020) used AI models for prediction of shifts of the shoreline in eastern Indian coast. A comparative study involving two Machine Learning (ML) approaches, that is, k-nearest neighbours (KNN), and support vector machine (SVM) and ANN were conducted to assess their respective performances. The study showed that the performance of the ANN model was superior relative to the KNN and the SVM with 86.2% accuracy.

Table 7. Validation of result compared with recent researches

Authors	Model	Performance indicator			
		RMSE	R	Accuracy	MAPE
Kumar *et al.* (2020)	ANN			0.862	
Yin *et al.* (2021)	SARIMA, NNAR, and LSTM		0.875		
Gomez-de la Pena *et al.* (2022)	LSTM and CNN	5 m			
Gomez-de la Pena *et al.* (2023)	CNN and CNN – LSTM	4.34	0.6		
Zeinali *et al.* (2021)	NARNET, NARXNET, RBF, GRNN, and TDNN				17.18
Adusumilli *et al.* (2024)	DNN	0.835			
Senechal and Coco (2024)	Feedforward ANN		0.82		
Calkoen *et al.* (2021)	ML - SimpleFFN, SimpleLSTM, DeepAR, MQCNN, DeepSSM				10
Montaño *et al.* (2020)	Hybrid ML-kNN, NARXNN, ANN, LSTM, RB, and BNN	0.991			
Proposed shoreline predictive model	NARXNN	0.04108	0.9906		

Yin *et al.* (2021), also used ML approaches to predict shorelines variations at Nha Trang using statistical forecasting model, Seasonal Auto-regressive Integrated Moving Average (SARIMA), Auto-Regressive Neural Network (ARNN), deep learning algorithm, as well as Long Short-Term Memory (LSTM). These were compared with predictions obtained from the conventional Empirical Orthogonal Function (EOF), and it was found that all the ML models performed better than EOF, with R > 0.875. Gomez-de la Pena *et al.* (2023), also investigated the ability of deep learning (DL) algorithms, that is convolutional neural networks (CNNs) and a hybrid CNN-LSTM networks, to predict inter annual shoreline positions in New Zealand using observations from camera system. The results were compared with two other numerical shoreline models, one based on the concept of equilibrium and the other a model that seeks to address issue of different timescales in shoreline drivers. The DL models were found to outperform the reference models and yielded more accurate and reliable predictions. Zeinnali *et al.* (2021), used an ANN to predict changes in the shoreline along the coast of Narrabeen in Australia using recurrent ANNs such as NARNN and NARXNN, and other methods including Radial Basis Function (RBF), Generalize Regression Neural Networks (GRNN), and Time Delay Neural Networks (TDNN). It was found that NARXNN yielded most accurate results, followed by the NARNN giving a reliable prediction of the shoreline with reference to existing data. Table 7 presents details on the validity of this study in relation to recent research.

Research Implications

Though shoreline change is a natural geomorphic process that varies with time, and the phenomenon is responsible for coastal landforms, alterations in wave climate and human interferences with coastal processes and ecosystems pose a significant threat to the livelihood and investments of coastal stakeholders. This is crucial for low-lying sandy beaches where the construction of new coastal structures such as harbours could to alter the natural sediment transport regime, particularly within the western zone of the Ghanaian coast. Therefore, it is imperative to know the shoreline change trends within the area so as to inform decision makers, Governments, local authorities, and Coastal planners and developers regarding future coastal development plans and mitigation strategies to be adopted in the event of flooding and coastal erosion. As a result, developing an AI model to predict Shoreline change in the study area is vital. The NARX model developed for predicting Shoreline change for sandy beaches can help governments and policymakers to formulate appropriate policies to combat coastal flooding and erosion of valuable coastal zones. The NAR Model, which performed slightly

weaker compared to the NARX, requires only the dependent variables for the prediction, and thus has economic advantage in shoreline prediction due to the high cost of acquiring high resolution shoreline dataset. This would lead to substantial improvements in coastal management and a better understanding of beach morphodynamics. It would also enable early detection and measurement of shoreline recession within vulnerable areas, thereby reducing the losses associated with coastal flooding. This is achievable because accurate shoreline change prediction is very useful for providing valuable information to forewarn coastal developers and stakeholders regarding their investments.

Conclusions

Shoreline position varies with time due to the effect of waves, tides as well as anthropogenic factors which interfere with coastal processes and ecosystems. In this study, we explored the use of Artificial Intelligence techniques in the prediction of shoreline change rate along the sandy beach of the western region of Ghana. The aim is to improve the accuracy and reliability of shoreline change prediction along sandy beaches. BPNN and two recurrent neural networks – NAR and NARX - models were trained using shoreline positions extracted from spatial data obtained between 1974 and 2020, and the results were compared with MLR. The experiment explores the effect of varying model inputs, loss function, and model parameters in a systematic manner. The accuracy of the prediction was measured by calculating the RMSE, PRMSE, RSR, ELM and R values. The R-value obtained for the BPNN was 0.9696 for training and 0.9723 for testing; while NAR yielded R-value of 0.983 for training and 0.982 for testing; the NARX gave R-value of 0.985 for training and 0.982 for testing compared with the MLR which gave a prediction with R value equals 0.561. The MSE for the BPNN, NARNN, NARXNN, and MLR are 0.0029, 0.00175, 0.0019 and 0.625 respectively. The recurrent NN algorithms (NAR and NARX) gave the optimum prediction of shoreline with the NARX performing slightly better than the NAR along the sandy beach of the Western Region of Ghana. This shows that the AI predicted both the linearity and the non-linearity in the complex nature of the shoreline dataset. This study confirms the findings of Calkoen *et al.* (2021), who observed that RNNs are a good fit for time-series forecasting.

Authors' Contributions

Conceptualization: C. B. B. and P. E. B.; Data curation: C. B. B. and P. B.; Formal analysis: P.B. and C. B. B; Methodology: C. B. B, P. E. B. and P. B.; Writing - original draft: C. B.B. and P. B.; Writing - review and editing: P.E.B. and P.B.

All authors read and approved the final manuscript.

Acknowledgments

This research received no specific grant from any funding agency in the public, commercial, or not-for-profit sectors. The authors are grateful to the University of Mines and Technology (UMaT) in Ghana for the assistance provided in the form of laboratory facilities during the study period.

The authors are grateful to the Lands Commission of Ghana for providing topographic data for the study. No funding was received from any agency for the conduct and publication of this study.

Conflict of Interests

The authors declare that there are no conflicts of interest related to this article.

References

Addo KA, Walkden M, Mills JT (2008). Detection, measurement and prediction of shoreline recession in Accra, Ghana. ISPRS Journal of Photogrammetry and Remote Sensing 63(5):543-558. *https://doi.org/10.1016/j.isprsjprs.2008.04.001*

Adusumilli S, Cirrito N, Engeman L, Fiedler JW, Guza RT, Lange AM, Merrifield MA, O'Reilly W, Young AP (2024). Predicting shoreline changes along the California coast using deep learning applied to satellite observations. Journal of Geophysical Research: Machine Learning and Computation 1(3):e2024JH000172. *https://doi.org/10.1029/2024JH000172*

Ahmed A, Khalid M (2017). Multi-step ahead wind forecasting using nonlinear autoregressive neural networks. Energy Procedia 134:192-204. *https://doi.org/10.1016/j.egypro.2017.09.609*

Alizadeh G, Vafakhah M, Azarmsa A, Torabi M (2011). Using an artificial neural network to model monthly shoreline variations. 2nd International Conference on Artificial Intelligence, Management Science and Electronic Commerce (AIMSEC) 4893-4896. *https://doi.org/10.1109/aimsec.2011.6010717*

Alvarez-Cuesta M, Toimil A, Losada IJ (2021). Reprint of: Modelling long-term shoreline evolution in highly anthropized coastal areas. Part 2: Assessing the response to climate change. Coastal Engineering 169:103985. *https://doi.org/10.1016/j.coastaleng.2021.103961*

Anim M (2019). Beach erosion: A study of cross-shore particle size characteristics and profile evolution along the Ghanaian coastline. Doctoral dissertation, University of Cape Coast. *https://ir.ucc.edu.gh/xmlui/handle/123456789/8590*

Ankrah J, Monteiro A, Madureira H (2023). Shoreline change and coastal erosion in West Africa: A systematic review of research progress and policy recommendation. Geosciences 13(2):59. *https://doi.org/10.3390/geosciences13020059*

Appeaning Addo K (2014). Managing shoreline change under increasing sea-level rise in Ghana. Coastal Management 42(6): 555-567. *https://doi.org/*10.1080/08920753.*2014.*964820

Armenio E, De Serio F, Mossa M, Petrillo AF (2019). Coastline evolution based on statistical analysis and modeling. Natural Hazards and Earth System Sciences 19: 937-1953. *https://doi.org/*10.5194/*nhess*-19-1937-2019

Ayyam V, Palanivel S, Chandrakasan S (2019). Coastal ecosystems and services. In: Coastal Ecosystems of the Tropics - Adaptive Management. Springer, Singapore. *https://doi.org/10.1007/978-981-13-8926-9_2*

Baig MRI, Ahmad IA, Shahfahad, Tayyab M, Rahman A (2020). Analysis of shoreline changes in Vishakhapatnam coastal tract of Andhra Pradesh, India: an application of digital shoreline analysis system (DSAS). Annals of GIS 26(4):361-376. *https://doi.org/*10.1080/19475683.2020.1815839

Barragán JM, De Andrés M (2015). Analysis and trends of the world's coastal cities and agglomerations. Ocean and Coastal Management 114:11-20. *https://doi.org/*10.1016/*j.ocecoaman*.2015.06.004

Boateng I (2012). An application of GIS and coastal geomorphology for large scale assessment of coastal erosion and management: A case study of Ghana. Journal of Coastal Conservation 16:383-397. *https://doi.org/*10.1007/s11852-012-0209-0

Boye CB, Appeaning Addo K, Wiafe G, Dzigbodi-Adjimah K (2018). Spatio-temporal analyses of shoreline change in the western region of Ghana. Journal of Coastal Conservation 22:769-776. *https://doi.org/*10.1007/s11852-018-0607-z

Boye CB, Baffoe PE, Ketibuah JN (2022). Assessment of shoreline change along the sandy beach of Ellembelle district of Ghana. Geoplanning: Journal of Geomatics and Planning 9(1):17-24. *https://doi.org/10.14710/geoplanning.9.1.17-24*

Bujak D, Bogovac T, Carević D, Ilic S, Lončar G (2021). Application of artificial neural networks to predict beach nourishment volume requirements. Journal of Marine Science and Engineering 9(8):786. *https://doi.org/*10.3390/jmse9080786

Calkoen F, Luijendijk A, Rivero CR, Kras E, Baart F (2021). Traditional vs. machine-learning methods for forecasting sandy shoreline evolution using historic satellite-derived shorelines. Remote Sensing 13(5):934. https://doi.org/10.3390/jmse9080786

Chen JC, Wang YM (2020). Comparing activation functions in modeling shoreline variation using multilayer perceptron neural network. Water 12(5):1281. https://doi.org/10.3390/w12051281

Defeo O, McLachlan A, Schoeman DS, Schlacher TA, Dugan J, Jones A, Lastra M, Scapini F (2009). Threats to sandy beach ecosystems: A review. Estuarine, Coastal and Shelf Science 8(1):1-12. *https://doi.org/*10.1016/j.ecss.2008.09.022

Dodo UA, Dodo MA, Husein MA, Ashigwuike EC, Mohammed AS, Abba SI (2024). Comparative study of different training algorithms in backpropagation neural networks for generalized biomass higher heating value prediction. Green Energy and Resources 2(1):100060. https://doi.org/10.1016/j.gerr.2024.100060

Evadzi PI, Zorita E, Hünicke B (2017). Quantifying and predicting the contribution of sea-level rise to shoreline change in Ghana: information for coastal adaptation strategies. Journal of Coastal Research 33(6):1283-1291. *https://doi.org/*10.2112/JCOASTRES-D-16-00119.1

Goh ATC (1995). Empirical design in geotechnics using neural networks. Geotechnique 45(4):709-714. *https://doi.org/*10.1680/*geot.*1995.45.4.709

Gomez-de la Peña E, Coco G, Whittaker C, Montaño J (2023). On the use of convolutional deep learning to predict shoreline change. Earth Surface Dynamics 11(6):1145-1160. *https://doi.org/*10.5194/esurf-11-1145-2023

He L, Kurita H, Wang Z, Narita F (2024). Structural optimization of PVDF cellular resonators for energy-harvesting enhancement based on backpropagation neural network and NSGA-II algorithm. Sensors and Actuators A: Physical 376:115608. *https://doi.org/*10.1016/j.sna.2024.115608

Hesamian G, Torkian F, Johannssen A, Chukhrova N (2024). A learning system-based soft multiple linear regression model. Intelligent Systems with Applications 22:200378. *https://doi.org/*10.1016/*j.iswa.*2024.200378

Huang Y, Xu W, Sukjairungwattana P, Yu Z (2024). Learners' continuance intention in multimodal language learning education: an innovative multiple linear regression model. Heliyon 10(6):e2810410. *https://doi.org/10.1016/j.heliyon.2024.e28104*

Jamei M, Bailek N, Bouchouicha K, Hassan MA, Elbeltagi A, Kuriqi A, Al-Ansari N, Almorox J, El-kenawy ESM (2023). Data-driven models for predicting solar radiation in semi-arid regions. Computers, Materials and Continua 74(1):1625-1640. *https://doi.org/*10.32604/*cmc.*2023.031406

Jeyanthi S, Subadra M (2014). Implementation of single neuron using various activation functions with FPGA. 2014 IEEE International Conference on Advanced Communications, Control and Computing Technologies, pp 1126-1131. *https://doi.org/10.1109/ICACCCT.2014.7019273*

Jonah FE, Mensah EA, Edziyie RE, Agbo NW, Adjei-Boateng D (2016). Coastal erosion in Ghana: Causes, policies, and management. Coastal Management 44(2):116-130. *https://doi.org/10.1080/08920753.2016.1135273*

Kesse GO (1986). Oil and gas possibilities on-and offshore Ghana. M 40: Future Petroleum Provinces of the World, pp 427-444.

Khairudin K, Ul-Saufie AZ, Senin SF, Zainudin Z, Rashid AM, Bakar NFA, Abd Wahid MZA, Azha SF, Abd-Wahab F, Wang L, Sahar F N (2024). Enhancing riverine load prediction of anthropogenic pollutants: harnessing the potential of feed-forward backpropagation (FFBP) artificial neural network (ANN) models. Results in Engineering 22:102072. *https://doi.org/*10.1016/*j.rineng.*2024.102072

Kumar L, Afzal MS, Afzal MM (2020). Mapping shoreline change using machine learning: a case study from the eastern Indian coast. Acta Geophysica 68(4):1127-1143. *https://doi.org/*10.1007/*s*11600-020-00454-9

Legates DR, McCabe GJ (2013). A refined index of model performance: a rejoinder. International Journal of Climatology 33(4):1053-1056. *https://doi.org/*10.1002/joc.3487

Luijendijk A, Hagenaars G, Ranasinghe R, Baart F, Donchyts G, Aarninkhof S (2018). The state of the world's beaches. Scientific Reports 8:6641. *https://doi.org/10.1038/s41598-018-24630-6*

Maio CV, Gontz AM, Tenenbaum DE, Berkland EP (2022). Coastal hazard vulnerability assessment of sensitive historical sites on Rainsford Island, Boston Harbor, Massachusetts. Journal of Coastal Research 28:20-33. *https://doi.org/10.2112/JCOASTRES-D-10-00104.1*

Martin P (2022). Linear regression: An introduction to statistical models. SAGE Publications.

Montaño-González J, Cancino M (2020). Exploring the relationship between language learning strategies and self-efficacy of Chilean university EFL students. Mextesol Journal 44(2):1-16.

Moussaid J, Fora AA, Zourarah B, Maanan M, Maanan M (2015). Using automatic computation to analyze the rate of shoreline change on the Kenitra Coast, Morocco. Ocean Engineering 102:71-77. *https://doi.org/10.1016/j.oceaneng.2015.04.044*

Nandy S, Singh R, Ghosh S, Watham T, Kushwaha SPS, Kumar AS, Dadhwal VK (2017). Neural network-based modelling for forest biomass assessment. Carbon Management 8(4):305-317. *https://doi.org/*10.1080/17583004.2017.1357402

Nassar K, Mahmod WE, Fath H, Masria A, Nadaoka K, Negm A (2019). Shoreline change detection using DSAS technique: Case of North Sinai Coast, Egypt. Marine Georesources and Geotechnology 37(1):81-95. *https://doi.org/10.1080/1064119X.2018.1448912*

Nayak SC, Misra BB, Behera HS (2014). Impact of data normalization on stock index forecasting. International Journal of Computer Information Systems and Industrial Management Applications 6:13-13. *www.mirlabs.net/ijcisim/index.html*

Oyedotun TD (2014). Shoreline geometry: DSAS as a tool for historical trend analysis. Geomorphological Techniques 3(2):1-12. *https://www.researchgate.net/publication/264534620*

Ozgoren M, Bilgili M, Sahin B (2012). Estimation of global solar radiation using ANN over Turkey. Expert Systems With Applications 39(5):5043-5051. *https://doi.org/*10.1016/*j.eswa.*2011.11.036

Rastgou M, He Y, Jiang Q (2024). Implementation and efficient evaluation of backpropagation network training algorithms in parametric simulations of soil hydraulic conductivity curve. Journal of Hydrology 636:131302. *https://doi.org/10.1016/j.jhydrol.2024.131302*

Rizkina MA, Adytia D, Subasita N (2019). Nonlinear autoregressive neural network models for sea level prediction, study case: In Semarang, Indonesia. Proceedings of the 7th International Conference on Information and Communication Technology (ICoICT), Kuala Lumpur, Malaysia, 24-26 July 2019, IEEE, pp 1-5. *https://doi.org/10.1109/ICoICT.2019.8835307*

Ruggiero P, List JH (2009). Improving accuracy and statistical reliability of shoreline position and change rate estimates. Journal of Coastal Research 25(5):1069-1081. *https://doi.org/10.2112/08-1051.1*

Saadon A, Abdullah J, Yassin IM, Muhammad NS, Ariffin J (2024). Nonlinear multi-independent variables in quantifying river bank erosion using neural network autoregressive exogenous (NNARX) model. Heliyon 10(4):e26252. *https://doi.org/10.1016/j.heliyon.2024.e26252*

Saba AI, Elsheikh AH (2020). Forecasting the prevalence of Covid-19 outbreak in Egypt using nonlinear autoregressive artificial neural networks. Process Safety and Environmental Protection 141:1-8. *https://doi.org/10.1016/j.psep.2020.05.029*

Sarkar R, Julai S, Hossain S, Chong WT, Rahman M (2019). A comparative study of activation functions of NAR and NARX neural network for long-term wind speed forecasting in Malaysia. Mathematical Problems in Engineering 1:6403081. *https://doi.org/10.1155/2019/6403081*

Schlacher TA, Jones AR, Dugan JE, Weston MA, Harris L, Schoema DS, Hubbard DM, Scapini F, Nel R, Lastra M, McLachlan A, Peterson CH (2014). Open-coast sandy beaches and coastal dunes. Coastal Conservation 19:37-92. *https://doi.org/*10.1017/CBO9781139137089.004

Senechal N, Coco G (2024). On the role of hydrodynamic and morphologic variables on neural network prediction of shoreline dynamics. Geomorphology 451:109084. *https://doi.org/10.1016/j.geomorph.2024.109084*

Shen Y, Peng Y, Shuai Z, Zhou Q, Zhu L, Shen ZJ, Shahidehpour M (2023). Hierarchical time-series assessment and control for transient stability enhancement in islanded microgrids. IEEE Transactions on Smart Grid 14(5): 3362-3374. *https://doi.org/*10.1109/*TSG.*2023.3237965

Sheremetov L, Cosultchi A, Martínez-Muñoz J, Gonzalez-Sánchez A, Jiménez-Aquino MA (2014). Xdata-driven forecasting of naturally fractured reservoirs based on nonlinear autoregressive neural networks with exogenous input. Journal of Petroleum Science and Engineering 123:106-119. *https://doi.org/*10.1016/*j.petrol.*2014.07.013

Thomas RC, Frey AE (2013). Shoreline change modeling using one-line models: General model comparison and literature review. www. *erdc-library.erdc.dren.mil*

Thomas RC, Frey AE (2013). Shoreline change modeling using one-line models: General model comparison and literature review. ERDC/CHL CHETNII-55. Vicksburg, MS: US Army Engineer Research and Development Center.

Tian Y, Nearing GS, Peters-Lidard CD, Harrison KW, Tang L (2016). Performance metrics, error modeling, and uncertainty quantification. Monthly Weather Review 144(2):607-613. *https://doi.org/10.1175/MWR-D-15-0087.1*

Ulger M, Tanrivermis Y (2023). Numerical modelling of shoreline changes based on the Preissmann scheme technique: a case study in Skarya province, Karasu district, Turkey. Ocean and Coastal Management 243:106752. *http://dx.doi.org/10.2139/ssrn.4330073*

Willmott CJ, Matsuura K (2006). On the use of dimensioned measures of error to evaluate the performance of spatial interpolators. International Journal of Geographical Information Science 20(1):89-102. *https://doi.org/10.1080/13658810500286976*

Yaw Dadson I (2015). Coastal erosion dynamics and landmass change along Cape Coast-Sekondi Coastline in Ghana. Doctoral dissertation, University of Cape Coast. *https://ir.ucc.edu.gh/xmlui/handle/123456789/6435*

Yin C, Anh DT, Mai ST, Le A, Nguyen VH, Nguyen VC, Tinh NX, Tanaka H, Viet NT, Nguyen LD, Duong TQ (2021). Advanced machine learning techniques for predicting Nha Trang shorelines. IEEE Access 9:98132-98149. *http://hdl.handle.net/123456789/6435*

Zeinali S, Dehghani M, Talebbeydokhti N (2021). Artificial neural network for the prediction of shoreline changes in Narrabeen, Australia. Applied Ocean Research 107:102362. *https://doi.org/10.1016/j.apor.2020.102362*

Zu X, Zhang Y (2022). Soybean and soybean oil price forecasting through the nonlinear autoregressive neural network (NARNN) and NARNN with exogenous inputs (NARNN–X). Intelligent Systems with Applications 13:200061. *https://doi.org/10.1016/j.iswa.2022.200061*

Tel.: +233244444179